

N 66-86101

Code - None
Pages - 56
TAX-54839

ELECTRON MICROPROBE STUDY OF THE JAJH DEH

KOT LALU ENSTATITE CHONDRITE

Klaus Keil¹ and Christian A. Andersen²

56p

ABSTRACT

Polished sections of the Jajh deh Kot Lalu enstatite chondrite have been studied microscopically. The composition of its minerals has been ascertained by means of local electron microprobe X-ray analysis. Well-analyzed minerals and pure elements were used as standards. Corrections were made for wavelength shift, detector deadtime, background, mass absorption, secondary fluorescence, and atomic number. Oxygen, nitrogen, and carbon were measured quantitatively using newly developed dispersive detection systems. The following minerals were found and analyzed: enstatite, pigeonite, oligoclase, kamacite, troilite, oldhamite, daubreelite, ferro alabandite, schreibersite, graphite, and a new mineral, sinoite (silicon oxynitride, $\text{Si}_2\text{N}_2\text{O}$). The unusual mineral association, the chalcophilic behavior of Ti, Mn, Cr, Ca, the occurrence of Si in kamacite, and the presence of sinoite indicate that the meteorite was formed under strongly reducing conditions. Chemical-mineralogical relationships between enstatite achondrites and enstatite chondrites are discussed. The results suggest that

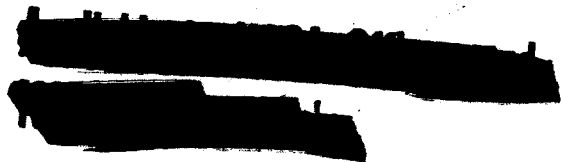
¹National Aeronautics and Space Administration, Space Sciences Division, Ames Research Center, Moffett Field, California.

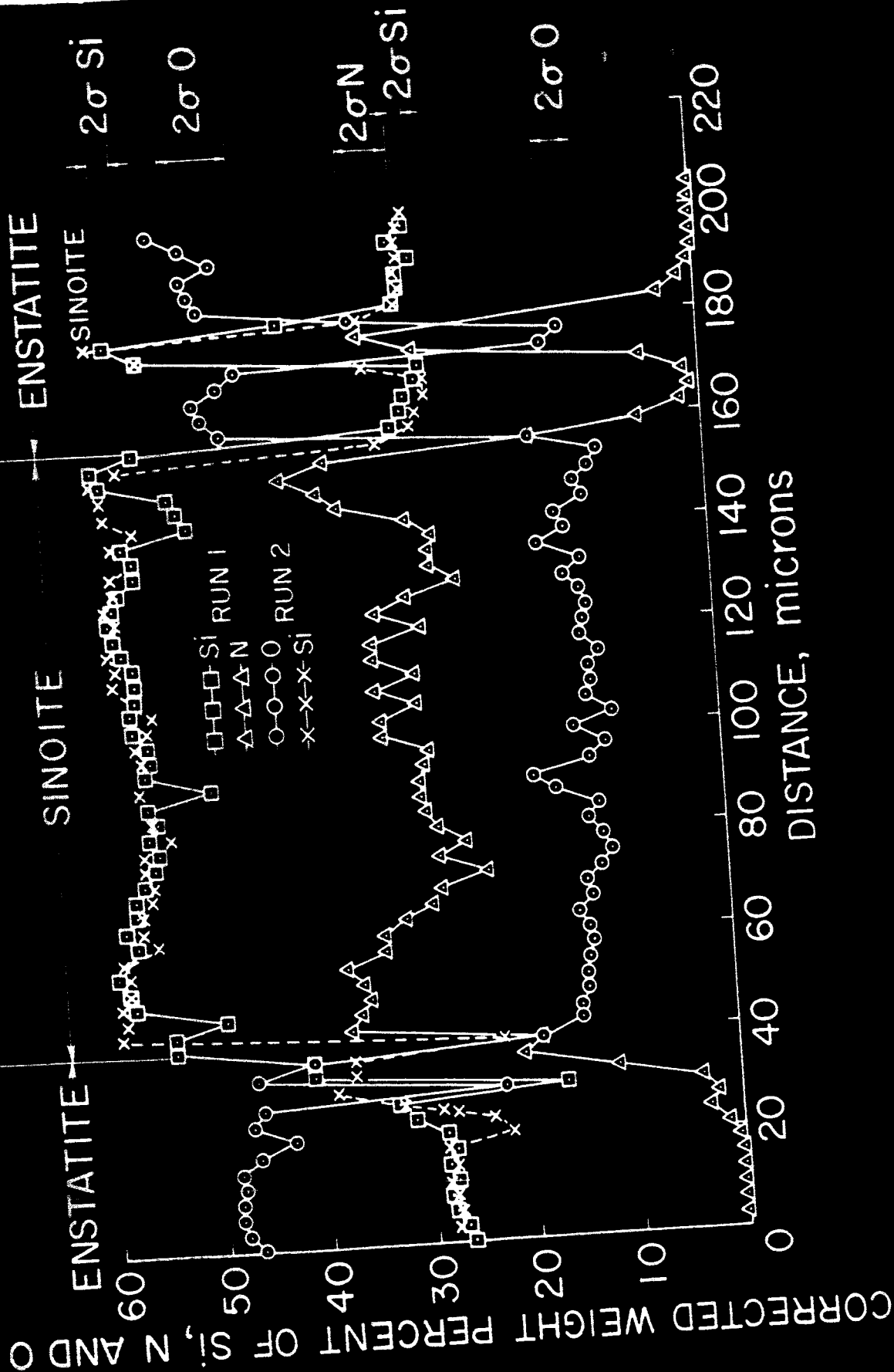
²Hasler Research Center, Applied Research Laboratories, Goleta, California.

enstatite achondrites may have originated via remelting of enstatite chondrite type stones with simultaneous gravitational separation under highly reducing conditions.

INTRODUCTION

Meteorites in general were formed under comparatively reducing conditions. However, among the various stone meteorite classes are two which were formed in an even higher reducing environment than were the majority of the ordinary stones. These are the enstatite achondrites and enstatite chondrites. Although small in number (only nine enstatite achondrites and twelve enstatite chondrites are known) they are of particular interest. Due to the highly reducing conditions, certain rare minerals were formed, most of which are unknown from terrestrial rocks. In the past, several of these meteorites and their minerals were studied microscopically (e.g., STORY-MASKELYNE, 1862, 1870; BORGSTRÖM, 1903; PRIOR, 1916; JOHNSTON and CONNER, 1922; LACROIX, 1923; FOSHAG, 1939, 1940; KUPLETSKII and OSTROVSKII, 1941; LONSDALE, 1947; BECK and LA PAZ, 1951; DAWSON et al., 1960; RAMDOHR, 1963). However, only very few quantitative analyses of minerals from these meteorites are available (e.g., BORGSTRÖM, 1903, FOSHAG, 1940; KEIL and FREDRIKSSON, 1963). The main reasons for the lack of quantitative analyses of these rare minerals are the difficulties involved in their clean mechanical separation from the complex intergrowths in the





meteorites as well as the limited quantities of meteoritic material available for destructive analysis. These difficulties can be overcome using electron microprobe techniques which allow non-destructive, quantitative analyses of mineral grains as small as one micron in diameter to be carried out both in polished and in thin sections.

The Jajh deh Kot Lalu enstatite chondrite was seen to fall on May 2, 1926 near the village of Jajh deh Kot Lalu, Faizganj taluk, Khairpur, Pakistan ($26^{\circ} 45' N$, $68^{\circ} 25' E$). Two fragments were recovered immediately after the fall, weighing 970 grams together. The only description was given by HOBSON (1927), who erroneously classified the meteorite as a veined crystalline chondrite; however, MASON (1962) listed the meteorite properly as an enstatite chondrite.

METHOD

The chemical compositions of the minerals in the Jajh deh Kot Lalu enstatite chondrite were determined by electron microprobe techniques. Polished sections of the meteorite were coated with an evaporated layer of carbon, a few hundred Angstroms thick to make them conductive. The electron microprobe permits nondestructive local chemical analysis of a volume of a few cubic microns of the surface regions of the sample. The sample is bombarded with a finely focused beam of high-energy electrons and the resultant

X-ray emission spectrum is analyzed for wavelength and intensity with dispersive X-ray detection systems. The measurements were carried out using three Applied Research Laboratory electron microprobe X-ray analyzers located at the University of California, La Jolla; at the Hasler Research Center, Goleta, California; and at the NASA Ames Research Center's Space Sciences Division, Moffett Field, California.

The chemical analyses of the minerals were performed in the following manner. Typical grains were optically selected and viewed while being bombarded by the electron beam. The ability to analyze and view a grain simultaneously assures an accurate correlation of chemical composition with the position of the beam on the sample. Three modes of analysis were used. First, qualitative spectra were taken of every mineral using a stationary electron beam and running the spectrometers through the complete wavelength ranges corresponding to elements of atomic numbers $Z = 5$ through 92 (boron through uranium). Second, scanning photographs of the mineral grains and their immediate surroundings were taken by sweeping the electron beam over a selected area in the sample and recording the resultant characteristic X-ray intensities as seen by the spectrometers on an oscilloscope screen (polaroid photographs of these images were taken and are presented in Figs. 1, 3, 6, 7, 11, 12, 14, and 16). Third, quantitative analyses of the elements known to be present in every mineral were carried out. Both pure

elements as well as chemically analyzed minerals were used as standards. The composition of the enstatite was evaluated using calibration curves given by KEIL and FREDRIKSSON (1964), while the pigeonite and oligoclase were analyzed using several chemically analyzed feldspar standards as well as pure Al and pure Fe. Iron and sulfur in the sulfides were measured with pure iron and a chemically analyzed pyrite as standards. Pure Mg (as well as enstatite and olivine), Ti, Cr, and Mn were used as standards in the analyses of the sulfides, while pure Fe, Ni, Co, and Si served to determine the composition of the metallic nickel-iron. Ca in the sulfides was compared with several Ca feldspars. Pure Fe, Ni, Co and a chemically analyzed apatite were used to analyze the schreibersite. The analyses of sinoite were performed with pure Si, SiO_2 , enstatite, and BN as standards. Both graphite and diamond were used as standards to determine the graphite in the meteorite.

The quantitative data were corrected for wavelength shift, detector deadtime, background, mass absorption, secondary fluorescence, and atomic number. Elements of atomic number 12 and above were corrected with the following data. Mass absorption corrections were carried out using mass absorption coefficients given in Norelco Reporter (1962) and the $f(X)$ tables given by ADLER (1962), while WITTENBERG'S (1962) formulas were used for secondary fluorescence corrections. The atomic number effect was empirically evaluated

by measuring the iron in FeS_2 of known composition against pure Fe. After all other corrections were carried out, the factor necessary to obtain the proper iron value for the FeS_2 relative to pure Fe was then used to correct the Mn, Cr, and Fe values in their respective sulfides relative to the pure metal standards.

In the course of the analysis of the new mineral sinoite ($\text{Si}_2\text{N}_2\text{O}$) discovered in this meteorite by electron microprobe analysis, nitrogen and oxygen were measured for the first time using the prototype detection systems developed at the Hasler Research Center employing an ultrathin window detector and analyzing crystals of large d spacings. Oxygen ($\text{O}_{K\alpha}$) was measured quantitatively using a KAP (potassium acid phthalate) crystal spectrometer, while nitrogen ($\text{N}_{K\alpha}$) was measured with the aid of a barium stearate monolayer crystal spectrometer. The detector was fitted with an ultrathin nitrocellulose window and was used for both $\text{O}_{K\alpha}$ and $\text{N}_{K\alpha}$ radiations. The quantitative analyses of silicon, nitrogen, and oxygen were performed by traversing the mineral grains with point-by-point integrations. This technique, also used for the analyses of the other minerals in the meteorite, was accomplished with a precision stepping motor which stepped the sample in 3 micron intervals under a stationary electron beam.

The above mentioned corrections were applied to correct the Si, N, and O values of the sinoite. It was found, however, that there was no measurable wavelength shift between mineral and

standards. The numbers for silicon, nitrogen, and oxygen obtained with 5 kv acceleration voltages were corrected for mass absorption by means of the experimental $f(X)$ curves given by GREEN (1962). The $C_{K\alpha}$ curve was used to correct the oxygen and nitrogen, while the $Al_{K\alpha}$ curve was used to correct the silicon. The mass absorption coefficients were taken from HENKE et al. (1957). The secondary fluorescence correction of $N_{K\alpha}$, calculated with WITTERT'S (1962) formulas, was found to be insignificant. The atomic number effect was corrected in the following way. The silicon and oxygen numbers of the mineral obtained with 5 kv accelerating voltages were compared with silicon and oxygen measurements of the surrounding enstatite, which is almost pure $MgSiO_3$. The values obtained by measuring enstatite were then compared to the silicon and oxygen numbers measured on quartz of constant composition. The correction factors necessary to obtain the proper silicon and oxygen values for SiO_2 , with enstatite as a standard, were then calculated after all the aforementioned corrections had been applied. These same factors were then used to correct the silicon and oxygen data of the mineral on the assumption that the atomic number effect for Si_2N_2O and SiO_2 is similar.

The precision of the measurements was found to be about 1 per cent of the amounts present. The accuracy depends upon the quality of the standards and is about 2 to 3 per cent of the amounts present. The precision of the nitrogen and oxygen values is about 10 per cent, while the accuracy is probably not better than

15 per cent of the amounts present, owing to the uncertainties in the mass absorption coefficients and the $f(\lambda)$ curves for the long wavelength.

RESULTS

Enstatite

The orthorhombic pyroxene enstatite is the most abundant mineral of the meteorite and makes up about 50-60 weight per cent of it. It is easily recognizable under the electron beam by its bright blue luminescence. It contains only 0.45% Fe and 0.52% Ca (Table 1) and, thus, is nearly pure magnesium orthosilicate. It sometimes occurs in euhedral crystals up to about 80 microns in length (Fig. 13).

Pigeonite

A pyroxene with higher calcium and iron contents is frequently observed on the boundaries between enstatite grains (Fig. 1). Its composition was determined by moving the sample in 2 micron steps under a fixed electron beam across the grain boundaries and measuring the composition quantitatively after each step. (A concentration-distance diagram is shown in Fig. 2.) The pyroxene contains 4.2% Ca and 1.3% Fe (Table 1); thus, it is properly named pigeonite.

Oligoclase

The meteorite contains about 10 per cent plagioclase. In polished sections this mineral is easily distinguished from enstatite by its lower reflectivity (Fig. 4), and by its reddish luminescence under electron bombardment. The plagioclase was found to contain 2.2% Ca (Table 1) and thus may properly be named oligoclase. It occurs in grains up to about 200 microns in diameter (Figs. 1, 4, and 6). Special care was taken to determine the iron content of the feldspar. Inclusion-free feldspar grains were selected optically as well as by using electron beam scanning images of up to 2000 times magnification. The iron content was determined in these grains and found to be 0.15 per cent.

Kamacite

About 20 per cent of the meteorite is metallic nickel-iron with an average nickel content of 5.87 per cent (Table 1). A remarkable feature of this kamacite is its silicon content of 0.95 per cent (Table 1; Figs. 1 and 11). The presence of silicon in the kamacite was first noted by PRIOR (1916) in the Khairpur enstatite chondrite. Similar amounts of silicon have been detected in other enstatite chondrites by RINGWOOD (1961). Together with the sulfides (Fig. 1) the kamacite occurs in xenomorphic grains that fill the spaces between the silicates (Fig. 4). In some instances, euhedral enstatite crystals are surrounded by kamacite,

the enstatite then obtrudes its euhedral outlines upon the kamacite (Fig. 13). Therefore, the kamacite can be considered to have crystallized last.

Graphite is characteristically associated with the kamacite, both in euhedral graphite crystals (Figs. 12 and 13) as well as in xenomorphic flakes enclosed in the kamacite (Fig. 11). Also, sinoite ($\text{Si}_2\text{N}_2\text{O}$) has occasionally been observed associated with the metal (Figs. 15 and 16).

As yet unexplained is the fact that the electron microprobe analyses of the kamacite do not add up to 100 per cent. The weight percentages of Fe, Ni, Co, and Si give only 98.69 per cent (Table 1); however, a large number of previous analyses of metallic nickel-iron with the same electron probe, same standards, and similar working conditions (KEIL and FREDRIKSSON, 1963; SHORT and ANDERSEN, 1964) always were very close to 100 per cent. The deviations from 100 per cent therefore seem not to be due to erroneous analyses. The only plausible explanation seems to be that about 1 to 1.5 per cent of some other elements are present. A qualitative spectrum taken on the kamacite showed no other elements present with atomic numbers $Z = 11 - 92$ (sodium through uranium) in amounts greater than about 0.1 per cent. The kamacite was also checked for elements with atomic numbers $Z = 5 - 9$ (boron through fluorine) but no such elements were detected. However, the sensitivity for these light elements in a metallic nickel-iron matrix

(high background) is low and possibly only amounts greater than a few per cent would have been seen. Therefore, it seems possible that the kamacite may contain about 1 - 1.5 per cent of some light elements in solid solution.

Troilite

About 5 per cent of the meteorite is troilite (FeS). The mineral occurs in xenomorphic grains frequently associated with metallic nickel-iron (Fig. 1). It usually exhibits exsolution lamellae of daubreelite and ferro alabandite (Figs. 1, 3, and 8-10). Sometimes troilite grains are surrounded by a thin (~5 microns) rim of oldhamite (Fig. 6).

The chemical composition of the mineral is given in Table 1. It was found to contain 0.69 per cent titanium and 0.65 per cent chromium. This is illustrated in electron beam scanning images (Figs. 1 and 3). The chalcophilic behavior of titanium was first noted in troilites from the Norton County achondrite (KEIL and FREDRIKSSON, 1963). Systematic study of other enstatite chondrites and enstatite achondrites always revealed the presence of this element in the troilite (KEIL and ANDERSEN, 1964b,c).

The chromium content of the troilite is interesting and agrees with the results of VOGEL and HEUMANN (1950) on the Fe-FeS-CrS-Cr phase diagram. These authors pointed out that whenever troilite is the parent substance for the (now exsolved) daubreelite, the troilite should retain a small amount of chromium.

Oldhamite

The mineral oldhamite (CaS) was discovered by STORY-MASKELYNE (1862, 1870) in the Bustee enstatite achondrite and has since been described from several other enstatite achondrites and enstatite chondrites. In the Jajh deh Kot Lalu enstatite chondrite it was found in irregularly shaped grains up to about 150 microns in size. While the other sulfides are rather homogeneously distributed throughout the meteorite, the oldhamite is highly enriched in certain regions. Figure 4 is a microphotograph of such an oldhamite rich region.

Troilite, daubreelite, and ferro alabandite, the other three sulfides occurring in the Jajh deh Kot Lalu enstatite chondrite, are closely associated in this meteorite (Figs. 1, 3, and 8-10). The main mass of the oldhamite, however, is usually separated from these minerals (Fig. 4). Where the oldhamite is found in contact with the other sulfides it forms individual grains (Figs. 1 and 4). In the sections investigated the oldhamite has never been observed as exsolution lamellae in troilite. Only once a "lamella" of daubreelite with some troilite has been observed in an oldhamite grain (Fig. 5). Rarely, oldhamite was found as a thin rim (~5 microns) surrounding larger troilite grains (Fig. 6).

The chemical composition of the oldhamite is given in Table 1 and illustrated in several electron beam scanning

images (Figs. 1 and 7). Besides the two major elements, calcium and sulfur, it contains 0.51% Mg, 1.01% Mn, and 0.44% Fe.

Daubreelite

Daubreelite (FeCr_2S_4) has been discovered by SMITH (1876) in the Coahuila iron meteorite and was later described from a number of other irons, particularly hexahedrites (e.g., HEIDE et al., 1932; PERRY, 1944). In iron meteorites it is always found closely associated with troilite. The Hvittis enstatite chondrite was the first stone meteorite where the mineral was observed (BORGSTRÖM, 1903). Since then it has been described from several other enstatite chondrites and enstatite achondrites (e.g., RAMDOHR, 1963; KEIL and FREDRIKSSON, 1963).

In the Jajh deh Kot Lalu enstatite chondrite the daubreelite occurs as exsolution lamellae in the troilite. The diameter of these lamellae may vary from a few microns to more than 100 microns, even within a single troilite grain (Figs. 1, 3, and 8-10). In enstatite chondrites the daubreelite generally is very closely associated with the troilite. This is contrary to its occurrence in enstatite achondrites, where it is found in isolated individual grains usually without association to troilite.

The daubreelite in the Jajh deh Kot Lalu enstatite chondrite was found to contain 16.5% Fe, 35.3% Cr, 44.4% S, and in addition, the minor elements of 2.38% Mn and 0.05% Ti (Table 1).

Ferro Alabandite

A manganese sulfide with a considerable iron content (no analysis given) was first described from the metallic iron bearing basalt from Bühl near Kassel, Germany (RAMDOHR, 1952). It was later found in a pyrrhotite inclusion of the phonolite from Fohberg near Oberschaffhausen, Germany (RAMDOHR, 1957) and was named "Eisenalabandin" (ferro alabandite).

The chemical composition of the manganese-iron sulfide found in the Jajh deh Kot Lalu enstatite chondrite suggests its identity with ferro alabandite. It was found to contain 45.8% Mn, 11.7% Fe, 37.4% S, and minor amounts of Mg (2.15 per cent), Ca (0.20 per cent), and Cr (0.55 per cent) (Table 1). Thus, the composition of this mineral is different from the ferromagnesian alabandite discovered in the Norton County achondrite (KEIL and FREDRIKSSON, 1963), which contains considerably more Mg (10 per cent) and somewhat more Fe (15.2 per cent).

The ferro alabandite of the present meteorite occurs in exsolution lamellae (Fig. 9) and cigar shaped bodies (Fig. 10) in the troilite. This is contrary to the appearance of the ferromagnesian alabandite in the Norton County enstatite achondrite, where it occurs in grains isolated from troilite. The ferro alabandite exsolution lamellae in the troilite of the Jajh deh Kot Lalu enstatite chondrite are always parallel to the daubreelite exsolution lamellae (Figs. 1, 3, and 8-10).

Graphite

Graphite has been observed in two types in the meteorite, both of them being associated with the metallic nickel-iron. One type occurs in xenomorphic flakes in the metallic nickel-iron (Fig. 11). The xenomorphic type is quite abundant and has been observed in many nickel-iron grains. The second type was observed in only one example and resembles what has been described in the literature as cliftonite. As early as 1863 ROSE suggested that the cubical graphite crystals occasionally found in iron meteorites may be pseudomorphs of graphite after diamond, a point of view that has been supported by many students of meteorites, although it has not yet been proven. So far, these pseudomorphs have only been observed in iron meteorites, although RAMDOHR (1963) described well-orientated lamellar aggregates of graphite from the Indarch enstatite chondrite, which he interprets as possible pseudomorphs after some cubic mineral. The occurrence of cliftonite in an enstatite chondrite would be quite significant with regard to the pressure history of the rock. It would indicate that at one time diamond may have been formed in it. Although the graphite crystal observed in the Jajh deh Kot Lalu enstatite chondrite resembles in its external shape the typical cliftonite pseudomorphs from iron meteorites, its cliftonite nature has been questioned by Frondel (private communication). Frondel pointed out that the cliftonites from iron meteorites are always characterized by typical preferred orientation of the graphite resulting in very definite

sectors with different optical orientations due to reflection dichroism and reflection birefringence. The crystal shown in Fig. 13 is also optically anisotropic in reflected light with symmetrical extinction but without sectors of different orientation.

The chemical composition of the graphite in the Jajh deh Kot Lalu enstatite chondrite determined by electron microprobe analysis using newly developed carbon detection systems was found to be essentially 100% C (Table 1).

Schreibersite

Schreibersite is an accessory mineral in the meteorite and is usually associated with metallic nickel-iron. It was occasionally found in large grains up to 300 microns in diameter (Fig. 14). Also it was noted as a thin rim around kamacite grains. It was found to contain 62.4% Fe, 22.4% Ni, 15.4% P, and 0.30% Co.

Sinoite

In the course of the electron microprobe study of the Jajh deh Kot Lalu enstatite chondrite a new mineral, a silicon-nitrogen-oxygen compound, was discovered (KEIL and ANDERSEN, 1964a). Newly developed oxygen and nitrogen detection systems were successfully applied to ascertain its composition with the electron probe. The results

of the quantitative microprobe analyses indicated a compound close to $\text{Si}_2\text{N}_2\text{O}$ in composition (Table 2). Almost simultaneously an account of synthetic $\text{Si}_2\text{N}_2\text{O}$ was published by BROSSET and IDRESTEDT (1964). These authors prepared the compound by heating a mixture of silicon and quartz powder in an atmosphere of nitrogen at 1450°C and found it to be orthorhombic with cell dimensions $a = 8.843 \text{ \AA}$; $b = 5.473 \text{ \AA}$; $c = 4.835 \text{ \AA}$. The silicon-nitrogen-oxygen compound from the Jajh deh Kot Lalu enstatite chondrite was therefore separated for X-ray diffraction and crystal optics studies and compared with data obtained from the synthetic $\text{Si}_2\text{N}_2\text{O}$. The compound from the Jajh deh Kot Lalu enstatite chondrite and the synthetic $\text{Si}_2\text{N}_2\text{O}$ were found to be practically identical (ANDERSEN et al., 1964). The name sinoite is proposed for the silicon oxynitride occurring as a natural mineral in the meteorite, this name being directly derived from its chemical composition.

Sinoite occurs in lath-like crystals up to about 200 microns in length, both in the silicate matrix of the meteorite as well as associated with metallic nickel-iron (Figs. 15 and 16). In the latter case the sinoite often obtrudes its shape upon the metallic nickel-iron. In thin sections the mineral is colorless with high birefringence and higher refractive indices than the surrounding enstatite. In polished sections it appears light gray and is distinctly different from the enstatite (Fig. 15).

During the electron microprobe analyses the exact position of the impingement of the electron beam on the mineral was observed as a distinctive greenish-yellow luminescence. The chemical composition of the mineral obtained by means of electron microprobe analysis is given in Table 2 in comparison to theoretical $\text{Si}_2\text{N}_2\text{O}$. The silicon values agree well, however, there is a slight difference in the oxygen and nitrogen values between sinoite and theoretical $\text{Si}_2\text{N}_2\text{O}$. These differences may in part be due to the uncertainties in the oxygen and nitrogen measurements (accuracy ± 15 per cent of the amount present). However, the fact that the nitrogen value is higher and the oxygen value is lower in the sinoite in comparison to theoretical $\text{Si}_2\text{N}_2\text{O}$ seems to suggest that the mineral may not have exactly stoichiometric composition but may really be somewhat richer in nitrogen and poorer in oxygen.

The quantitative chemical composition of the mineral was obtained by moving the polished section in steps of 3 microns under a stationary electron beam and carrying out quantitative analyses after every step. An example of such a one-dimensional chemical profile is given in Fig. 17. It was taken along track B of Fig. 16. In this profile two separate traverses were made, one giving simultaneous analyses of silicon and nitrogen, and the other giving simultaneous analyses of silicon and oxygen. The same line of traverse was attempted on both runs. On a micron scale, however, duplication of exactly the same point of integration is extremely difficult. This is indicated in Fig. 17 by the slight differences in the two silicon profiles. This also accounts for the fact that the silicon,

nitrogen, and oxygen numbers obtained in the two different runs do not always add up to 100 per cent. Similar traverses have been taken on several other grains with essentially the same results.

The following conclusions may be drawn from Fig. 17:

- a. It is apparent that the composition of the grain away from the grain boundaries is, on a micron scale, rather homogeneous and variations are usually within the precision of the method as indicated by the 2σ values. This was also observed in all the other grains of the mineral analyzed. This is particularly demonstrated by the only slight variations in the silicon values. In addition, the average silicon, nitrogen, and oxygen values for these regions in different grains agree well within the precision of the method. Not too much should be read into the various minor fluctuations of the nitrogen and oxygen values in areas with almost constant silicon contents. Such things as surface irregularities and relief may possibly influence the long wavelength considerably.
- b. In some instances the fluctuations of the silicon, nitrogen, and oxygen values clearly exceed the precision of the method, which is illustrated by the 2σ values in Fig. 17. A decrease in the silicon and nitrogen values sometimes parallels an increase in the oxygen (ANDERSEN et al., 1964). The identity of the apparently silicon- and

nitrogen-poor and oxygen-rich phase is unknown except that enstatite (MgSiO_3) has been eliminated as a result of the absence of magnesium. Further work is in progress.

- c. There seems to be a tendency of a slight enrichment of oxygen toward the grain boundaries of the mineral. This can be seen in the $O_{K\alpha}$ image of Fig. 16. Similar observations have been made on other grains (ANDERSEN et al., 1964).

The mineral has been separated from the meteorite for further studies by crushing a 5-gram piece of the stone and fractionating the powder in methylene-iodine-acetone mixtures of different densities (ANDERSEN et al., 1964). Sinoite was found to be concentrated in the 2.80 - 2.85 density fraction. This indicates that its density is close to that calculated for $\text{Si}_2\text{N}_2\text{O}$. The refractive indices were measured by the immersion method and found to be $\alpha = 1.740$, $\gamma = 1.855$ (mean refractive index of synthetic $\text{Si}_2\text{N}_2\text{O} = 1.79$). The closeness of γ and β indicates that the mineral is optically negative. The crystals are length-slow, i.e., $\gamma = c$. X-ray diffraction patterns were taken of sinoite and found to be identical with those obtained from synthetic $\text{Si}_2\text{N}_2\text{O}$. However, slight differences in the intensities of certain X-ray diffraction lines in sinoite and synthetic $\text{Si}_2\text{N}_2\text{O}$ may indicate that the sinoite is not exactly stoichiometric $\text{Si}_2\text{N}_2\text{O}$, but, in agreement with the microprobe analyses, somewhat richer in nitrogen, poorer in oxygen.

DISCUSSION

The rather unusual mineral assemblage of the Jajh deh Kot Lalu enstatite chondrite and the composition of these minerals indicates that the meteorite was formed under extremely reducing conditions. This is suggested by the low ferrous iron content (0.45 per cent) of the enstatite in the presence of some 20 per cent metallic nickel-iron as well as in the absence of the oxygen richer Fe-Mg silicate olivine. The high degree of reduction is also apparent in the chalophilic tendencies exhibited by elements of ordinarily lithophilic character, such as Ti, Cr, Mn, Mg, and Ca, as well as by the occurrence of Si in solid solution in the metallic nickel-iron. The occurrence of sinoite ($\text{Si}_2\text{N}_2\text{O}$) together with tridymite* in the meteorite further indicates that there was not sufficient oxygen available to bind all the excess silicon as SiO_2 .

The occurrence of the new mineral sinoite ($\text{Si}_2\text{N}_2\text{O}$) seems to be of particular significance for the specific and extraordinary environment in which this rock was formed. Unfortunately there are no thermodynamic data available on this compound. A discussion of its conditions of formation is therefore limited at the present time. The compound has been synthesized by heating a silicon and quartz powder in a nitrogen atmosphere at 1450°C (BROSSET and IDRESTEDT, 1964).

*Tridymite was not observed in this specimen of Jajh deh Kot Lalu but was identified by X-ray diffraction and crystal optics studies carried out by B. Mason on crushed and density separated fractions of other specimens of the same meteorite (ANDERSEN et al., 1964).

It seems possible that the compound in the meteorite may have formed in a similar process from SiO_2 in a highly reducing environment, where nitrogen was available.

Of particular significance is the similarity in the mineralogy of enstatite chondrites and enstatite achondrites. The chemical-mineralogical relationships between these two groups will be discussed in more detail elsewhere (KEIL and ANDERSEN, 1964b,c). However, some of the relationships that became apparent in the present study will be discussed briefly.

It was suggested by RINGWOOD (1961), MASON (1962), LOVERING (1962), KEIL and FREDRIKSSON (1963), MORGAN and LOVERING (1964), and others that enstatite achondrites may have been derived via remelting of enstatite chondrite type stones with simultaneous gravitational separation under highly reducing conditions. This suggestion is supported by the results of the present study.

The two meteorite groups are quite different in their bulk chemical compositions; these differences being largely due to the loss of Fe, Ni, and S in the enstatite achondrites in comparison to enstatite chondrites. This can be interpreted by gravitational separation of most of the metallic nickel-iron, troilite, and the other sulfides from the enstatite chondrite type parent material. However, the mineralogy of the two groups is quite similar, although there are considerable differences in the amounts of the heavy minerals as well as in the textures of the two groups. Both

contain the same minerals, among them rare compounds like ferro alabandite, daubreelite, oldhamite, etc. Even nitrogen compounds are present in both types ($\text{Si}_2\text{N}_2\text{O}$ in the Jajh deh Kot Lalu enstatite chondrite, TiN in the Bustee enstatite achondrite). Textural and structural differences may be interpreted in the light of the above mentioned hypothesis. While the enstatite chondrites are usually dark, dense rocks with or without chondrules, the enstatite achondrites are coarse grained and light in color. In the enstatite chondrites daubreelite and ferro alabandite often form exsolution lamellae in the troilite, while in the enstatite achondrites these minerals occur in individual grains frequently separated from each other.

The highly reducing environment is characteristic of both groups. Particularly significant are the Ti contents of the troilite. The enstatite chondrites have troilite with about 0.6% Ti without much variation from grain to grain and from meteorite to meteorite. In the enstatite achondrites, however, the Ti content varies from grain to grain and frequently exceed several per cent. This effect may be due to progressive enrichment of Ti in the iron sulfide remaining in the achondrites during the course of the gravitational separation under highly reducing conditions (KEIL and ANDERSEN, 1964b,c). That the gravitational separation occurred under highly reducing conditions is further indicated by the low nickel contents of the kamacite in enstatite achondrites

(~3.5 per cent) compared to the higher nickel content in the metal of enstatite chondrites (~6 per cent). This difference may be due to a reduction of the minor amounts of divalent iron, known to be present in silicates of enstatite chondrites, to the metal phase in the process of remelting (KEIL and FREDRIKSSON, 1963). The considerable amounts of graphite present in enstatite chondrites and its apparent absence in enstatite achondrites seem to indicate that the graphite (among others) may have acted as a reducing agent in the process of remelting the enstatite chondrite material and thus was lost.

However, the problem of crystallization of enstatite directly from a melt of approximately enstatite composition remains still unsolved (FOSHAG, 1940).

Systematic electron microprobe studies of the other enstatite chondrites and enstatite achondrites are presently in progress and will be reported elsewhere.

ACKNOWLEDGEMENTS

We thank Dr. Brian Mason for suggesting this meteorite for investigation and supplying the sample, and Drs. Gustaf Arrhenius and Kurt Fredriksson for the opportunity to perform the early microprobe measurements at the La Jolla microprobe laboratory. This study was supported in part by a National Academy of Sciences - National Research Council Resident Research Associateship to K. Keil.

REFERENCES

- ADLER I. (1962) Electron probe absorption tables. U. S. Dept. Interior, Geological Survey, Washington 25, D. C.
- ANDERSEN C. A., KEIL K. and MASON B. (1964) Silicon oxynitride, a meteoritic mineral. Science, 146, no. 3641, 256-257.
- ANONYMOUS (1962) Table of X-ray mass absorption coefficients. Norelco Reporter.
- BECK C. W. and LA PAZ L. (1951) The Nortonite fall and its mineralogy. Amer. Mineral, 36, 45-59.
- BORGSTRÖM L. H. (1903) Die Meteoriten von Hvittis und Marjalahti. Bull. Comm. Geol. Finlande, 14, 80 p.
- BROSSET C. and IDRESTEDT I. (1964) Crystal structure of silicon oxynitride, $\text{Si}_2\text{N}_2\text{O}$. Nature, 201, no. 4925, 1211.
- DAWSON K., MAXWELL I. A. and PARSONS D. E. (1960) A description of the meteorite which fell near Abee, Alberta, Canada. Geochim. et Cosmochim. Acta, 26, 251-262.
- FOSHAG W. F. (1939) Petrology of the Shallowater meteorite. Amer. Mineral, 24, 185.
- FOSHAG W. F. (1940) The Shallowater meteorite, a new aubrite. Amer. Mineral, 25, 779-786.
- GREEN M. (1962) Target absorption correction in X-ray microanalysis. III International Symp. X-ray Optics and X-ray Microanalysis, Stanford Univ., (H. H. Pettee, V. E. Cosslett, and A. Engström, eds.) Academic Press, 1963, 361-377.

- HEIDE F., HERSCHKOWITSCH E. and PREUSS E. (1932) Ein neuer Hexaedrit von Cerros del Buey Huerto, Chile. Chem. d. Erde, 7, 483-502.
- HENKE B. L., WHITE R. and LUNDBERG B. (1957) Semiempirical determination of mass absorption coefficient for the 5-50 Å X-ray region. J. Appl. Phys., 28, 98-105.
- HOBSON G. V. (1927) Six recent Indian aerolites. Geol. Surv. India, 60, 128-152.
- JOHNSTON R. A. A. and CONNOR M. F. (1922) The Blithfield meteorite. Trans. Roy. Soc. Canada, 16, 187-193.
- KEIL K. and ANDERSEN C. A. (1964a) Electron microprobe study of the Jajh deh Kot Lalu enstatite chondrite. Trans. Amer. Geophys. Union, 45, 86.
- KEIL K. and ANDERSEN C. A. (1964b) On the chalcophily of titanium in enstatite chondrites and enstatite achondrites (abstract). Annual Meeting of the Electrochemical Society, Symp. on the Electron Microprobe, Oct. 12-15, 1964, Washington, D. C.
- KEIL K. and ANDERSEN C. A. (1964c) On the geochemistry of titanium in stone meteorites. J. Geophys. Res. (in preparation).
- KEIL K. and FREDRIKSSON K. (1963) Electron microprobe analysis of some rare minerals in the Norton County achondrite. Geochim. et Cosmochim. Acta, 27, 939-947.
- KEIL K. and FREDRIKSSON K. (1964) The Fe, Mg and Ca distribution in coexisting olivines and rhombic pyroxenes of chondrites. J. Geophys. Res., 69, no. 16, 3487-3515.

- KUPLETSKII B. M. and OSTROVSKII I. A. (1941) The microscopic study of the meteorites of the USSR. The stony meteorite Staroe Pesyanoe. Meteoritika, 1, 59-62.
- LACROIX A. (1923) La composition de la météorite tombée a Saint-Sauveur (Haute-Garonne) en 1914. Compt. rend. Paris, 177, 561-565.
- LONSDALE J. T. (1947) The Pena Blanca Springs meteorite, Brewster County, Texas. Amer. Mineral., 32, 354-364.
- LOVERING J. F. (1962) The evolution of the meteorites - evidence for the coexistence of chondritic, achondritic, and iron meteorites in a typical parent meteorite body. Researches on Meteorites, (C. B. Moore, ed.), John Wiley and Sons, Inc. 179-197.
- MASON B. (1962) Meteorites. John Wiley and Sons, Inc., New York, 274 p.
- MORGAN J. W. and LOVERING J. F. (1964) Uranium and thorium abundances in stony meteorites. 2. The achondritic meteorites. J. Geophys. Res., 69, 1989-1994.
- PERRY S. H. (1944) The metallography of meteoric iron. Bull. U. S. Nat. Museum, 184, 206 p.
- PRIOR G. T. (1916) The meteoritic stones of Launton, Warbreccan, Cronstad, Daniel's Kuil, Khairpur, and Soko-Banja. Mineral Mag., 18, 1-25.
- RAMDOHR P. (1952) Neue Beobachtungen am Bühleisen. Sitz. Ber. Berliner Akad. Wiss., math.-naturw. Kl., 9-24.

- RAMDOHR P. (1957) Eisenalabandin, ein merkwürdiger natürlicher Hochtemperatur - Mischkristall. N. Jb. Min., 91, 89-93.
- RAMDOHR P. (1963) The opaque minerals in stony meteorites. J. Geophys. Res., 68, 2011-2036.
- RINGWOOD A. E. (1961) Silicon in the metal phase of enstatite chondrites and some geochemical implications. Geochim. et Cosmochim. Acta, 25, 1-13.
- ROSE G. (1863) Beschreibung und Einteilung der Meteoriten auf Grund der Sammlung im mineralogischen Museum zu Berlin. Abh. Akad. Wiss., Phys.-math. Kl., Berlin, p. 161.
- SHORT J. M. and ANDERSEN C. A. (1964) Nickel diffusion gradients in metallic meteorites and their cooling history. Trans. Amer. Geophys. Union, 45, 86.
- SMITH J. L. (1876) Aragonite on the surface of a meteoric iron, and a new mineral (daubreelite) in the concretions of the interior of the same. Amer. J. Sc., 12, 107-110.
- STORY-MASKELYNE N. S. (1862) On Aerolites. Dept. Brit. Ass. Adv. Sc., 32, 188-191.
- STORY-MASKELYNE N. S. (1870) On the mineral constituents of meteorites. Phil. Trans. Roy. Soc. London, 160, 189-214.
- VOGEL R. and HEUMANN T. (1950) Über Daubreelit. N. Jb. Min., Monatshefte, no. 8, 175-190.
- WITTRY D. B. (1962) Fluorescence by characteristic radiation in electron probe microanalysis. Univ. Southern California, Tech. Rep. 84-204.

Table 1.- Results of the electron microprobe analyses of minerals found in the Jajuh deh Kot Lulu enstatite chondrite (in weight per cent).

Mineral	C	H	O	Hg	Al	Si	Fe	Ca	Mg	Co	Pb	Ba	Th	U	Total
Enstatite	0.30	1.00	---	21.3	---	0.10	0.52	0.02	---	---	0.15	---	---	< 0.03	---
Pyroxene	---	---	---	22.5	---	0.15	4.2	0.02	---	---	1.3	---	---	---	---
Olivine	---	---	---	0.09	0.23	---	---	---	0.04	0.06	0.15	---	---	---	---
Pyroxene*	0.30	1.00	---	0.03	0.03	0.10	0.03	0.02	(0.1)	(0.1)	0.15	---	---	5.37	93.63
Trillite*	0.30	---	---	(0.02)	0.02	0.23	(0.2)	0.60	0.65	---	6.30	---	---	(0.1)	100.15
Olivine*	0.30	---	---	0.53	0.02	3.3	94.2	(0.2)	< 0.03	---	0.43	---	---	(0.2)	99.35
Pyroxene*	0.30	---	---	(0.03)	0.06**	43.4	(0.2)	0.05	35.4	---	16.5	---	---	(0.2)	93.63
Pyroxene*	0.30	---	---	25.15	0.03	16.4	0.30	0.02	0.03	---	11.7	---	---	(0.2)	97.30
Trillite*	---	---	---	(0.03)	(0.02)	(0.2)	(0.2)	(0.2)	(0.2)	---	(0.2)	---	---	(0.2)	100.00
Enstatite	---	---	---	---	---	---	---	---	---	---	0.30	---	---	(0.2)	100.5
Trillite*	0.30	31.5	13.1	(0.02)	(0.2)	(0.2)	(0.2)	(0.2)	(0.2)	(0.2)	(0.2)	(0.2)	(0.2)	(0.2)	101.2

*Spectrum scans were made of these minerals covering elements of atomic numbers 12 through 92. Numbers in parentheses are from spectrum scans; all other numbers are from point integration analyses. The upper limit of concentration of unlabeled elements is about 0.2 per cent.

**High limit of detectability is due to fourth-order Gr_K interference.

Note: Broken balance value not determined.

Table 2.- Composition of silicon oxynitride from the Jajh deh
Kot Lalu enstatite chondrite as obtained by electron
microprobe techniques (5 kv) in comparison to theoretical
 $\text{Si}_2\text{N}_2\text{O}$ (weight per cent).

Element	Silicon oxynitride from Jajh deh Kot Lalu	$\text{Si}_2\text{N}_2\text{O}$ theoretical composition
Si	56.6	56.1
N	31.5	27.9
O	13.1	15.9
Total	101.2	99.9

FIGURE CAPTIONS

Fig. 1(a).- Jajh deh Kot Lalu enstatite chondrite. Electron beam scanning pictures of complex mineral assemblage (Tr - troilite, Daub. - daubreelite, Old - oldhamite, Fe alab - ferro alabandite, NiFe - metallic nickel-iron, En - enstatite, Pig - pigeonite, Olig - oligoclase, A to D are tracks of quantitative analyses). The BSE (backscattered electron) image is a measure of the average atomic number (the brighter the image, the higher the average atomic number) and reveals surface irregularities. Pictures marked Fe, Ni, Si, and Ti were taken using the $K\alpha$ wavelengths of these elements. The Si content of the metallic nickel-iron and the Ti content of the troilite are remarkable (continues with Fig. 1(b)).

Fig. 1(b).- Jajh deh Kot Lalu enstatite chondrite. Electron beam scanning pictures of complex mineral assemblage (same area as in Fig. 1(a)). Pictures marked Mn, Mg, Cr, Al, Ca, and S were taken with the $K\alpha$ wavelengths of these elements. Oligoclase is recognized by its high Al content; the daubreelite (Cr image) does not contain Al. The apparent Al content in the Al image is due to fourth-order $CrK\beta$ radiation. A thin rim of pigeonite between enstatite and NiFe is recognized in the Ca image. The ferro alabandite is characterized by its high Mn content.

Fig. 2.- Jajh deh Kot Lalu enstatite chondrite. Quantitative Fe, Ca, and Mg analyses along track B of Fig. 1(a) (corrected weight per cent). The analyses were carried out by moving the sample in 2 micron steps under a fixed-electron beam and integrating after each step. The measurements were taken coming from metallic nickel-iron (high Fe) over a small oldhamite grain (Ca - peak) into pigeonite (Mg - peak) and again into oldhamite (high Ca). The pigeonite composition (shown in Table 1) was obtained by evaluating several of these tracks.

Fig. 3.- Jajh deh Kot Lalu enstatite chondrite. Electron beam scanning pictures of titanium bearing troilite with ferro alabandite and daubreelite exsolution lamellae. BSE is back-scattered electron image. Fe, Cr, Mn, S, and Ti are pictures taken with the $K\alpha$ wavelengths of these elements. The daubreelite is recognized by its Cr content, the ferro alabandite by its Mn content. The homogeneous distribution of the Ti in the troilite is apparent. Some nickel-iron (very bright image, upper right corner of BSE image) and enstatite (black in BSE image) are present.

Fig. 4.- Jajh deh Kot Lalu enstatite chondrite. Polished section, reflected light. Photomicrograph of oldhamite rich area. Oldhamite (gray grains with high relief); nickel-iron (white); troilite (light gray, together with nickel-iron); enstatite (gray main matrix); feldspar (deep dark areas in enstatite matrix).

Fig. 5.- Jajh deh Kot Lalu enstatite chondrite. Polished section, reflected light. Photomicrograph of oldhamite (center, gray, high relief) with bands of daubreelite (light gray) and troilite (white). Several other oldhamite grains (upper right corner, and center, near the edge) and troilite grains (light gray) are also shown. Dark gray matrix is enstatite.

Fig. 6.- Jajh deh Kot Lalu enstatite chondrite. Electron beam scanning pictures of troilite with rim of oldhamite. BSE is backscattered electron image. $\text{Ca}_{K\alpha}$, $\text{Al}_{K\alpha}$, $\text{S}_{K\alpha}$, $\text{Si}_{K\alpha}$, $\text{Mg}_{K\alpha}$, and $\text{O}_{K\alpha}$ are pictures taken in the $K\alpha$ wavelengths of these elements. The thin rim (~ 4 microns) of oldhamite around troilite is recognized in the $\text{Ca}_{K\alpha}$ and $\text{S}_{K\alpha}$ images. Troilite is white in the BSE image and shows up in the $\text{S}_{K\alpha}$ image. Feldspar is characterized by its Ca and Al contents. The lower part of the picture is enstatite, characterized by its Mg, Si, and O contents. The $\text{O}_{K\alpha}$ image was taken using prototypes of newly developed dispersive detection systems.

Fig. 7.- Jajh deh Kot Lalu enstatite chondrite. Electron beam scanning pictures of oldhamite in an enstatite matrix. BSE is backscattered electron image. Ca, Mn, S, Fe, and Mg are pictures taken with the $K\alpha$ wavelengths of these elements. The outlines of the oldhamite grain are shown in the BSE, Ca, Mn, and S images. The dark lines in the BSE image of the oldhamite are cracks. Areas with high Mg contents are enstatite. The bright areas in the Fe image are troilite and nickel-iron.

Fig. 8.- Jajh deh Kot Lalu enstatite chondrite. Polished section, reflected light. Photomicrograph of troilite (main mass) with daubreelite exsolution lamellae (light gray) of various thicknesses. Dark matrix is enstatite.

Fig. 9.- Jajh deh Kot Lalu enstatite chondrite. Polished section, reflected light. Photomicrograph of troilite (main mass) with ferro alabandite (dark gray) and daubreelite (light gray) exsolution lamellae parallel to each other. White is metallic nickel-iron (upper left corner and lower edge). Dark matrix is enstatite.

Fig. 10.- Jajh deh Kot Lalu enstatite chondrite. Polished section, reflected light. Photomicrograph of troilite (main mass) with daubreelite (light gray) and cigar shaped bodies of ferro alabandite (dark gray) associated with it. Surrounding matrix is enstatite (dark).

Fig. 11.- Jajh deh Kot Lalu enstatite chondrite. Electron beam scanning pictures of graphite flakes enclosed in metallic nickel-iron. BSE is backscattered electron image. C, Fe, Si, and S are pictures taken in the $K\alpha$ wavelengths of these elements. The graphite flakes are recognized in the C image. The $C_{K\alpha}$ image was taken using newly developed barium stearate pseudocrystal detection systems. The metallic nickel-iron is bright in the BSE image and contains some Si (Si image). Some troilite occurs adjacent to the metallic nickel-iron (S image), but does not contain graphite. The matrix surrounding the metallic nickel-iron and troilite (dark in BSE) is enstatite and feldspar, respectively.

Fig. 12.- Jajh deh Kot Lalu enstatite chondrite. Electron beam scanning pictures of (pseudomorph?) graphite associated with metallic nickel-iron and troilite in an enstatite and feldspar matrix. BSE is backscattered electron image. C, Fe, and Si are pictures taken in the $K\alpha$ wavelengths of these elements. In BSE the graphite is black, nickel-iron and troilite are white, and enstatite and feldspar show intermediate intensities. The graphite is recognized in the C image. The $C_{K\alpha}$ image was taken using newly developed barium stearate pseudocrystal detection systems. Metallic nickel-iron and troilite are distinguished in the lower left corner of the Fe image due to higher Fe intensities on the nickel-iron. The enstatite and feldspar matrix is bright in the Si image.

Fig. 13(a).- Jajh deh Kot Lalu enstatite chondrite. Polished section, reflected light. Photomicrograph of graphite (cf. Fig. 12), possibly a pseudomorph after a cubic mineral (center, gray), associated with nickel-iron and troilite (white) in enstatite and feldspar matrix (gray main mass). Euhedral enstatite crystal at the lower right corner of the graphite obtrudes its shape upon the metallic nickel-iron.

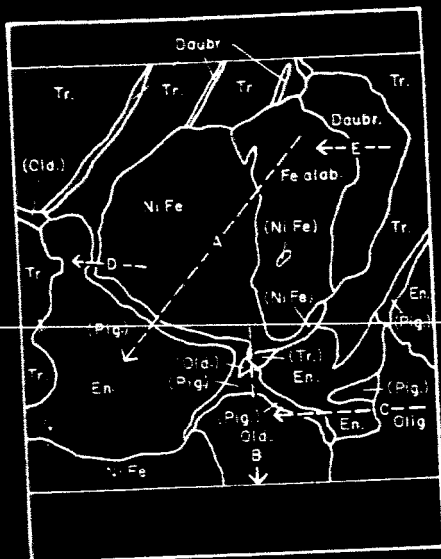
Fig. 13(b).- Jajh deh Kot Lalu enstatite chondrite. Polished section, reflected light. Photomicrograph of the same area as in Fig. 13(a), but with crossed polarizers. The graphite appears to be anisotropic with symmetric extinction.

Fig. 14.- Jajh deh Kot Lalu enstatite chondrite. Electron beam scanning pictures of schreibersite, associated with nickel-iron, in enstatite matrix. $\text{Fe}_{K\alpha}$, $\text{Ni}_{K\alpha}$, $\text{P}_{K\alpha}$, $\text{Mg}_{K\alpha}$, and $\text{Si}_{K\alpha}$ are pictures taken in the $K\alpha$ wavelengths of these elements. The schreibersite is characterized by its high Ni and P contents.

Fig. 15.- Jajh deh Kot Lalu enstatite chondrite. Polished section, reflected light. Photomicrograph of sinoite (center, light gray) associated with nickel-iron (white), ferro alabandite (left, light gray), enstatite (gray main mass).

Fig. 16.- Jajh deh Kot Lalu enstatite chondrite. Electron beam scanning pictures of sinoite ($\text{Si}_2\text{N}_2\text{O}$), associated with metallic nickel-iron and enstatite. $\text{Fe}_{L\alpha}$, $\text{Si}_{K\alpha}$, $\text{O}_{K\alpha}$, and $\text{N}_{K\alpha}$ are pictures taken in the $K\alpha$ wavelengths of these elements. The $\text{N}_{K\alpha}$ and $\text{O}_{K\alpha}$ images were taken using newly developed dispersive detection systems. The sinoite is characterized by its high Si and N contents. The $\text{O}_{K\alpha}$ image shows slight enrichments of O on the grain boundaries of the sinoite. The quantitative measurements plotted in Fig. 16 were carried out along track B. The triangular shape of the sinoite grain on the left side of the $\text{Si}_{K\alpha}$ image is remarkable. The matrix surrounding the sinoite is enstatite ($\text{Si}_{K\alpha}$ and $\text{O}_{K\alpha}$ image). The metallic nickel-iron is characterized by its high Fe content ($\text{Fe}_{L\alpha}$ image). The apparent $\text{N}_{K\alpha}$ intensities on the metallic nickel-iron and on the enstatite are due to high background values at this wavelength.

Fig. 17.- Jajh deh Kot Lalu enstatite chondrite. Quantitative Si, N, and O microprobe analyses of the silicon oxynitride grain shown in Fig. 16, track B. Quantitative analyses were performed by traversing the grains with point-by-point integration 3 microns apart.



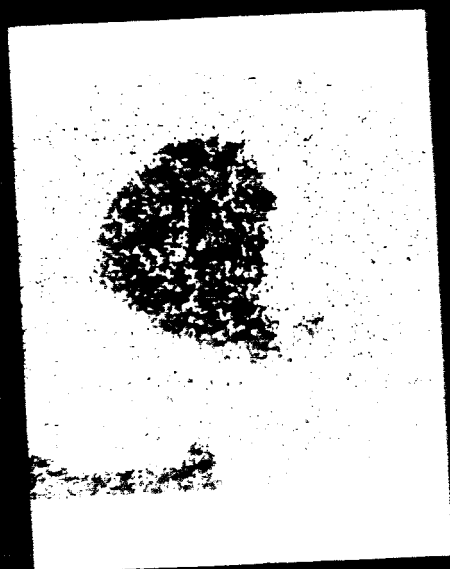
Sketch of grain boundaries



BSE



Fe



Ni



Si



Ti

50 μ

1A



Mn



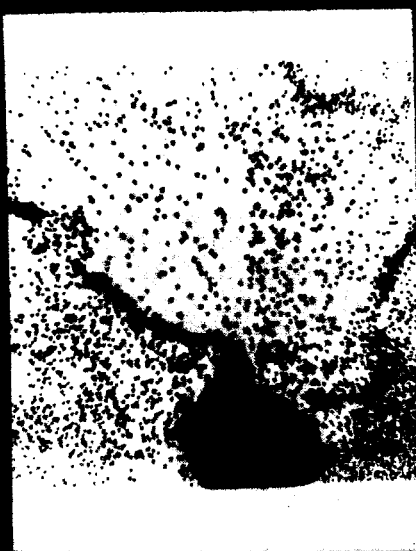
Mg



Cr



Li



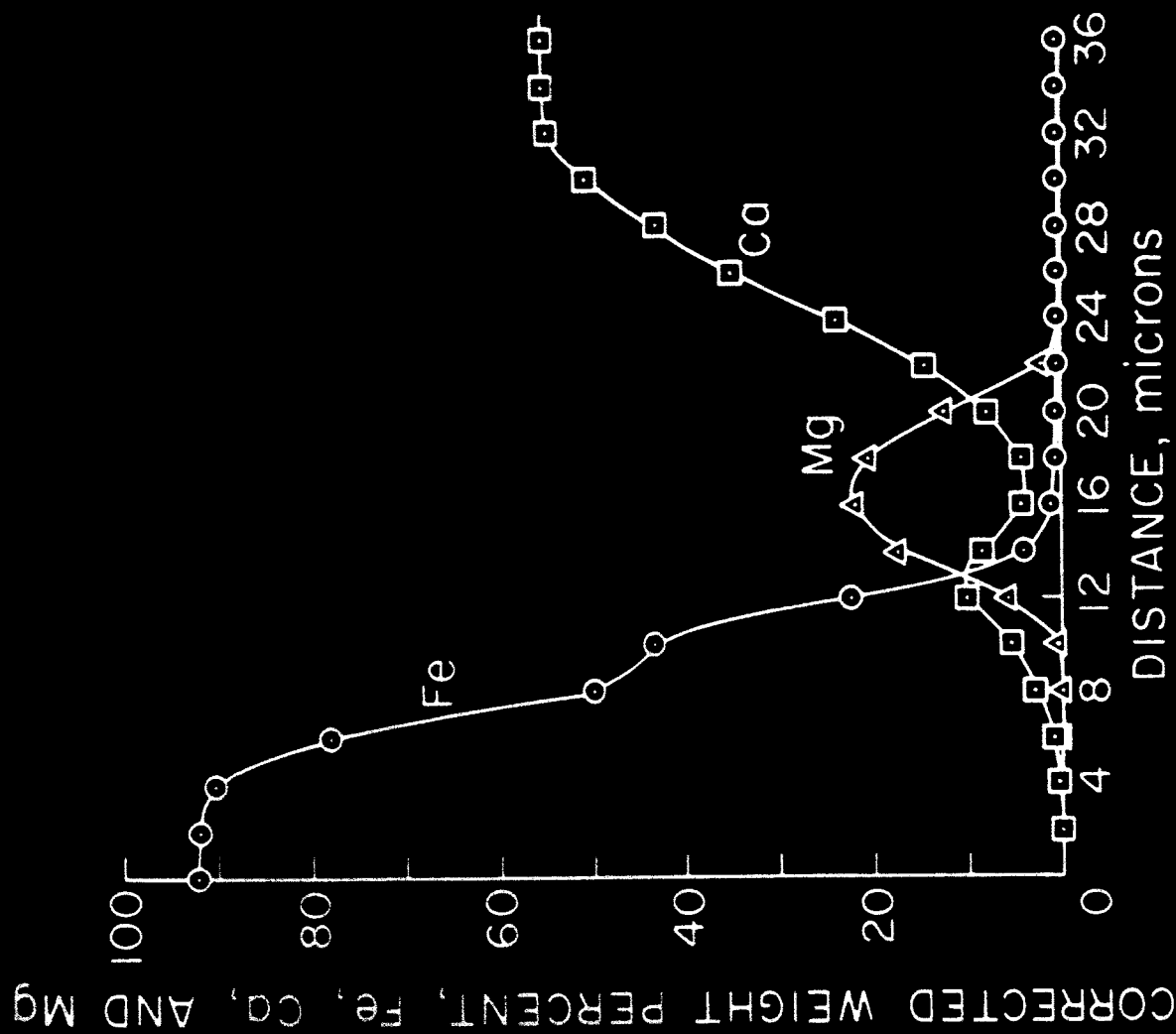
Co



Si

50μ

1E

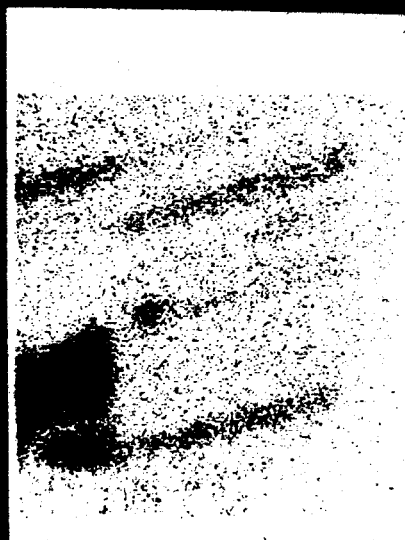




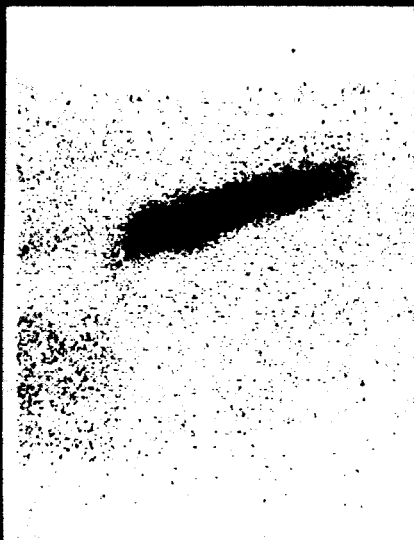
BSE



Fe



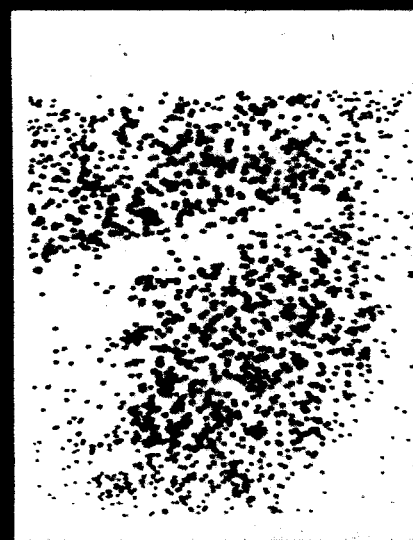
Cr



Mn

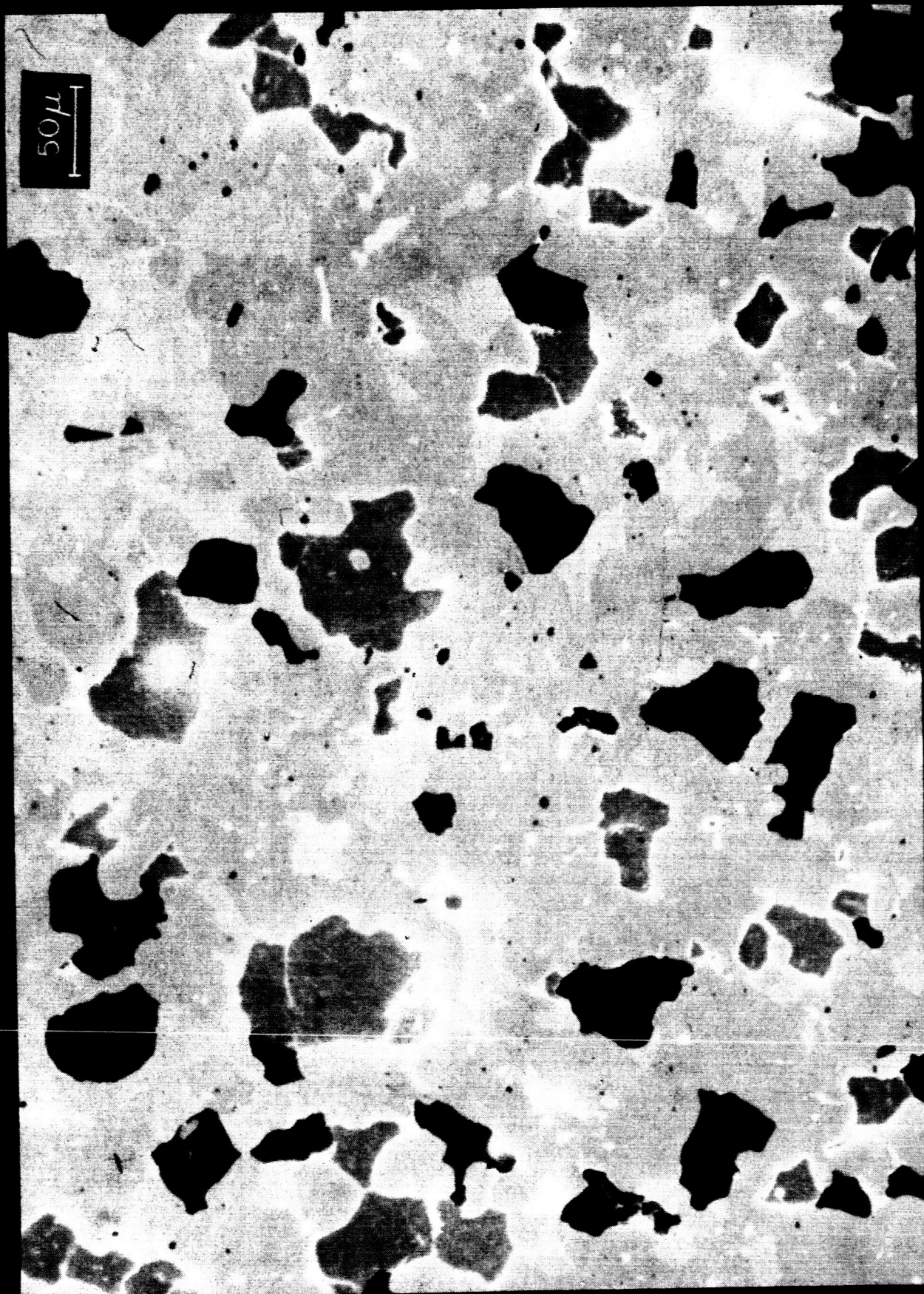


S



Ti

50μ





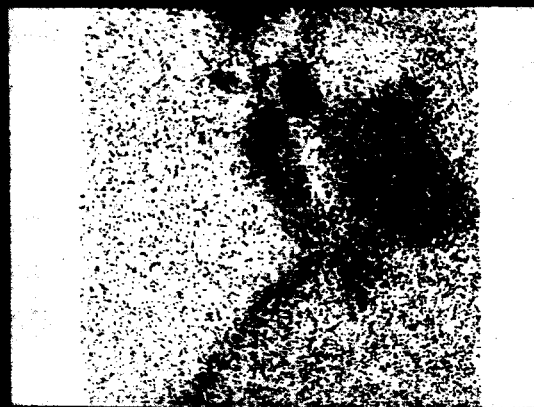
5



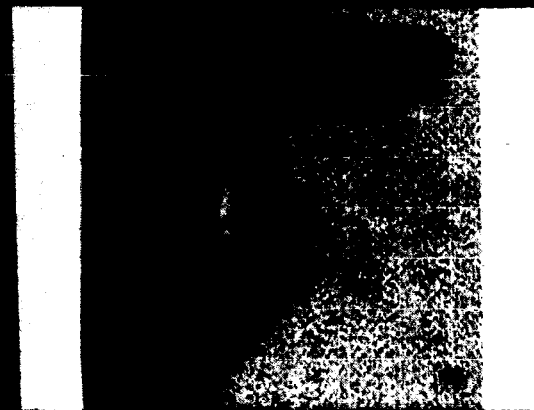
$U_{K\alpha}$



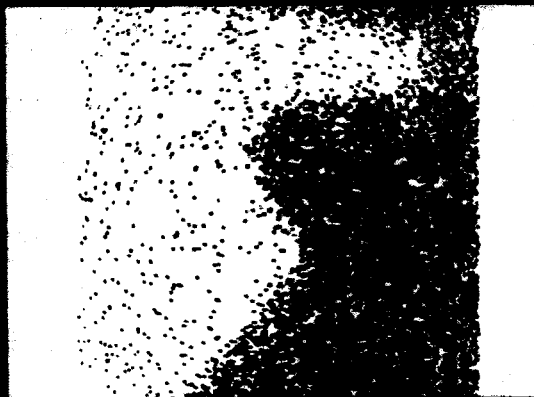
$A_{K\alpha}$



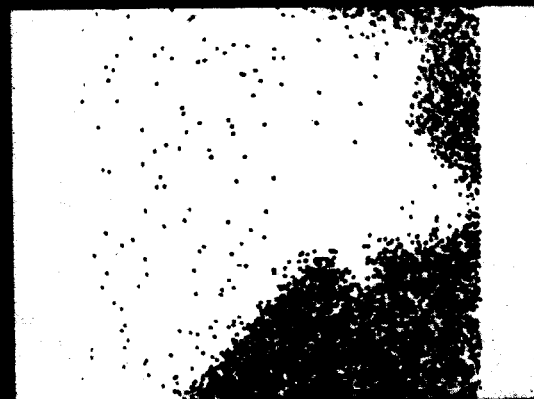
$Co_{K\alpha}$



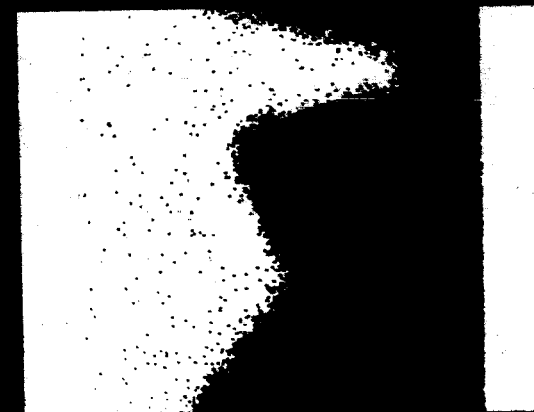
RSE



$O_{K\alpha}$



$Mq_{K\alpha}$



$Si_{K\alpha}$

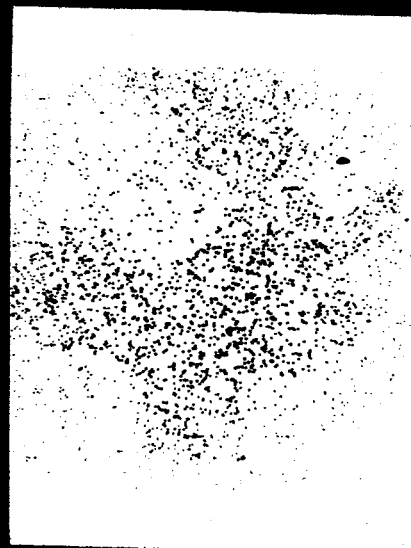
10 μ



BSE



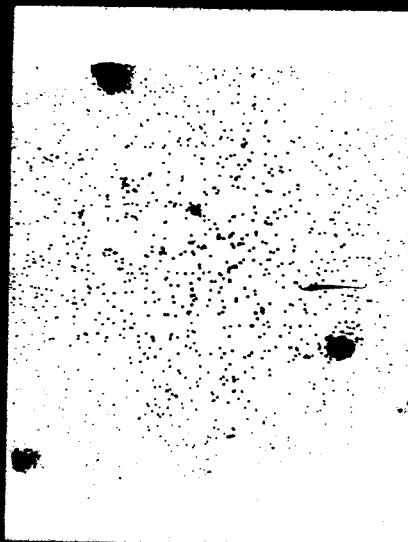
Co



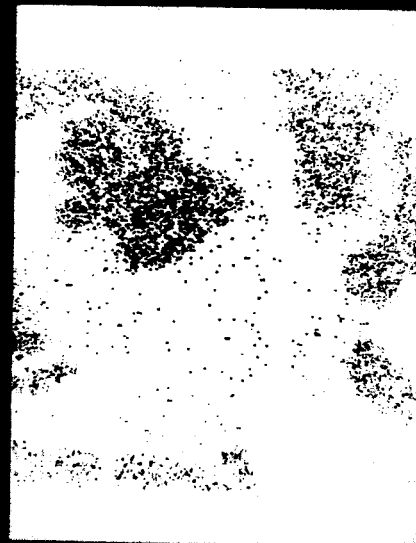
Mn



S



Fe



Mg

50 μm

8



50μ

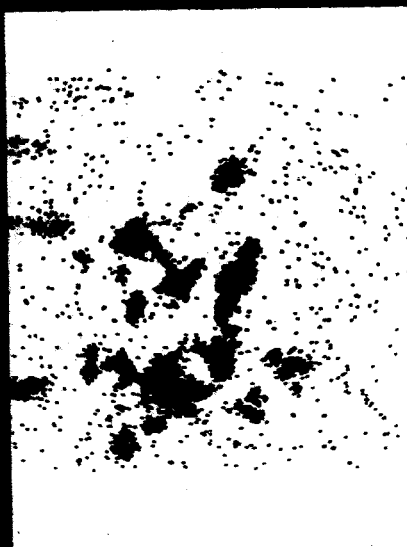




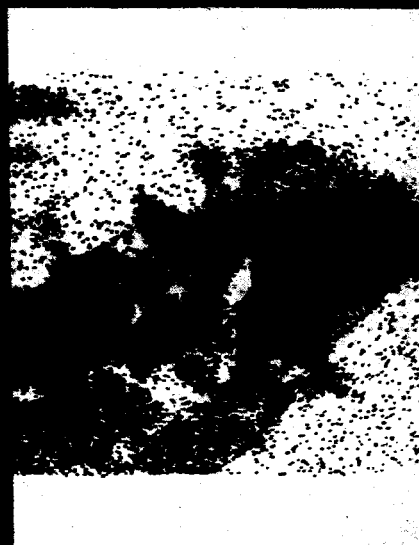
10



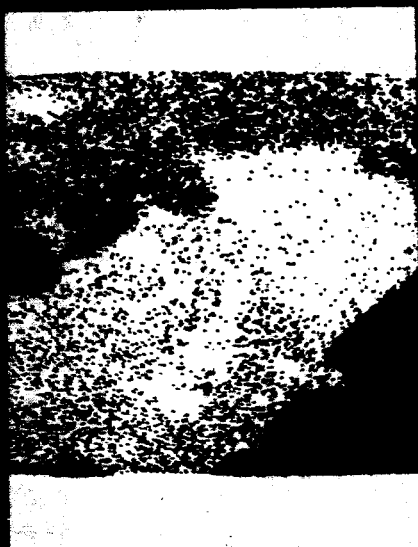
BSE



C



Fe



Si

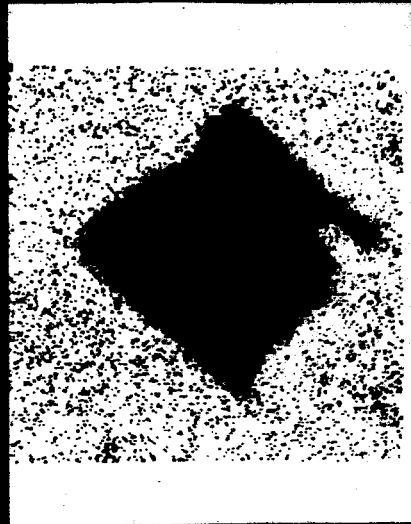


S

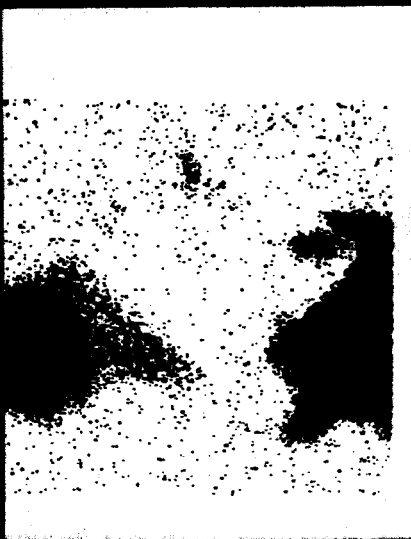
//



BSE



C



Fe



S

50 L

50 μ

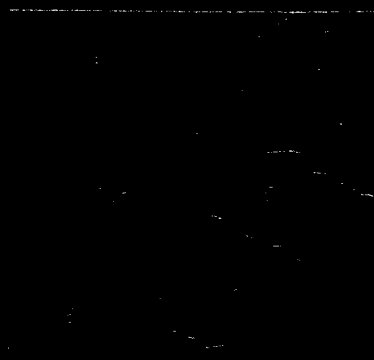
13A



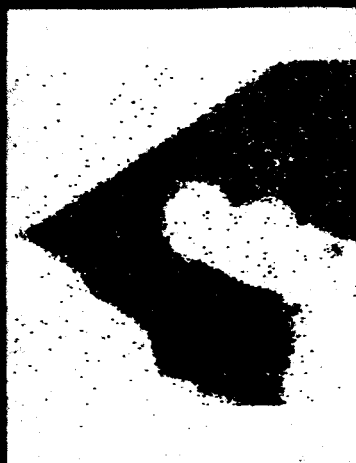
50μ

13B

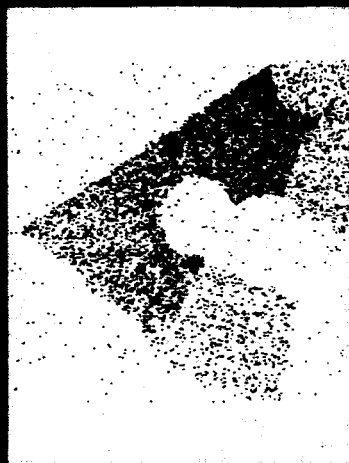




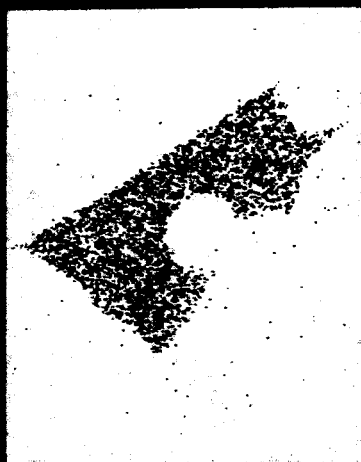
SKETCH OF GRAIN
BOUNDARIES



$\text{Fe}_{K\alpha}$



$\text{Ni}_{K\alpha}$



$\text{P}_{K\alpha}$



$\text{Mg}_{K\alpha}$



$\text{S}_{K\alpha}$

25L

14



25 μ

15



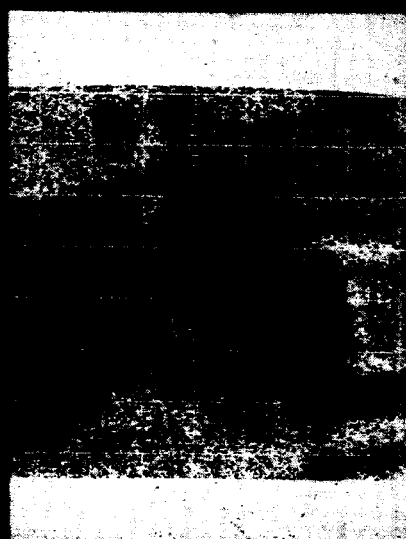
Fe₂O₃



SiO₂



Fe₂O₃



Fe₂O₃

50x

16